Biophysical Chemistry 161 (2012) 29–38

Contents lists available at SciVerse ScienceDirect

Biophysical Chemistry

journal homepage: http://www.elsevier.com/locate/biophyschem

Studying salt effects on protein stability using ribonuclease t1 as a model system ☆

David L. Beauchamp, Mazdak Khajehpour *

Department of Chemistry, University of Manitoba, Winnipeg, Manitoba, R3T 2N2, Canada

HIGHLIGHTS

► This work analyzes salt effects in the model enzyme Ribonuclease t1.
► Salt ions located at the protein-water interface induce image charges of the same sign in the low dielectric protein medium.
► We demonstrate that interactions between salt ions and their induced point charges majorly contribute to protein stability.

GRAPHICAL ABSTRACT

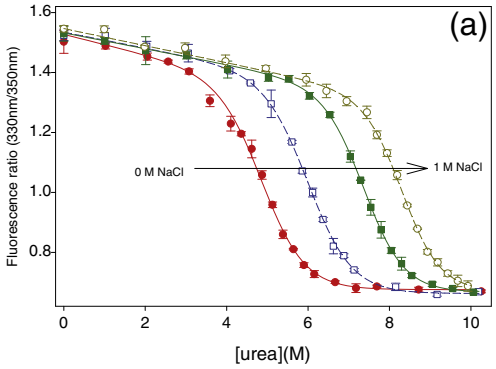

ARTICLE INFO

Article history:
Received 12 October 2011
Received in revised form 22 November 2011
Accepted 22 November 2011
Available online 2 December 2011

Keywords:
Salt effects
Protein folding
Fluorescence
Salting-out
Kirkwood interactions

ABSTRACT

Salt ions affect protein stability in a variety of ways. In general, these effects have either been interpreted from a charge solvation/charge screening standpoint or they have been considered to be the result of ion-specific interactions with a particular protein. Recent theoretical work suggests that a major contribution to salt effects on proteins is through the interaction of salt ions that are located near the protein surface and their induced point image charges that are located in the low-dielectric protein cavity. These interactions form the basis of "salting-out" interactions. Salt ions induce an image charge of the same sign in the low dielectric protein medium. The interaction between the induced charge and its mirror charge is repulsive and consequently thermodynamically destabilizing. However, a folded protein that has a much smaller surface area will be less destabilized than the unfolded state. Consequently, the folded state will be stabilized relative to the unfolded state. This work analyzes salt effects in the model enzyme ribonuclease t1, and demonstrates that interactions between salt ions and their induced point charges provide a major contribution to the observed salt-induced increase in protein stability. This work also demonstrates that in the case of weakly-binding ions (ions with binding constants that are in the order of 50 M^{-1} and less), salting-out effects should still be considered in order to provide a more realistic interpretation of ion binding. These results should therefore be considered when salt effects are used to analyze electrostatic contributions to protein structure or are used to study the thermodynamics of proteins associated with halophillic organisms.

1. Introduction

Salts are an essential component of living systems. In most systems the concentrations of ionic species such as sodium, potassium and chloride within extracellular and intracellular fluids vary between 1 and 200 mM [1]. At these concentrations, salts can have a sizable

☆ This work was supported in part by the University of Manitoba UMRG funding.
* Corresponding author. Tel.: +1 204 272 1546.
E-mail address: khajehpo@cc.umanitoba.ca (M. Khajehpour).

0301-4622/$ – see front matter © 2011 Elsevier B.V. All rights reserved.
doi:10.1016/j.bpc.2011.11.004

impact on the stability of biomolecules. In the case of highly charged polyelectrolytes such as nucleic acids, the highly negative net charge can destabilize conformations [2]. The presence of a salt can screen these repulsive interactions and increasing the ionic strength of the aqueous solvent stabilizes nucleic acid conformations in solution [2]. The building blocks of proteins are more diverse than those of nucleic acids and the net charge of proteins is much lower than that of nucleic acids of comparable size. The effect of salt on protein conformation and stability is therefore much more complex than that on nucleic acids, and differs in various proteins [3,4].

Perhaps the first systematic studies of salt effects on proteins were done by Hofmeister in the late nineteenth century [5]. In these studies Hofmeister discovered that the addition of salt decreases the solubility or "salts-out" the protein, and, that the efficacy of salting-out depends on the nature of the salt. The tabulation of these results led to the now ubiquitous "Hofmeister salt series" for protein stabilization. Subsequently, Kirkwood and Tanford applied a more rigorous statistical mechanical analysis to the salting-out problem [6,7]. In their analysis, the protein is modeled as a low-dielectric sphere with embedded charges. Based on their analysis, the existence of charges in the protein and ions in the solvent will have following effects on the protein–water system. First, a charge placed in a high dielectric medium (water) will induce an image charge of the same sign in the low dielectric medium (protein). The interaction between the charge and its image is unfavorable, adding salt will increase the number of unfavorable interactions causing protein aggregation — this phenomenon has been called "salting-out". Second, charged residues that are already placed within the low dielectric protein medium will induce an image charge of opposite sign in the high dielectric aqueous solvent medium; the interaction between charged protein residues and their image charges in the high dielectric solvent is thus favorable. The addition of salt can increase the magnitude of favorable interactions between charged protein residues and their image charges in the high dielectric solvent leading to an enhancement in protein solubility as the salt concentration is increased, this effect will be called "salting-in" — this "salting-in" is different from the effects of chaotropes such iodide and thiocyanate. However, because proteins have limited numbers of charges and large surface areas, at high enough concentrations of salt the number of salt ions near the protein surface will exceed the number of charged protein residues and lead to a preponderance of unfavorable interactions. These unfavorable interactions can be minimized by protein aggregation and precipitation, thus causing the protein molecules to always salt-out of solution at high enough salt concentrations.

Salts can also stabilize the folded relative to the unfolded states of proteins via the same interaction principles. Increasing salt concentration magnifies salting-out interactions. However, because the unfolded state has a larger surface area than the folded state, salting-out interactions will destabilize the unfolded state to a larger extent than the folded state. This leads to a net increase in the folding free energy of the protein. Increasing salt concentrations also stabilize salting-in interactions for both the folded and unfolded states: in the unfolded state, the charged residues can be modeled as point charges, adding salt increases the solvation energy of the point charges and screen charge–charge interactions; in the Kirkwood model of the folded state, salts increase the solvation energy of the sum of protein charges and screen the interactions that exist between charges embedded in the low dielectric protein medium.

In the last two decades, vast improvements in computational methodologies have led to great advances in our understanding of the electrostatic properties of proteins. Based on this sizable body of work, currently we have a better understanding of a variety of electrostatic biophysical phenomena such as the nature of charge solvation and charge interactions in proteins and the effects of salts on these interactions. The mechanism of the effects of salts on the pKa of charges residues [8–10] and how salts affect the strength of salt-bridges [11,12] in proteins is now much better understood. This being said, it is interesting that although salting-in and salting-out effects are one of the oldest observed phenomena in the field of protein–salt interactions, the nature of these effects is still not well understood. Most theoretical studies on Hofmeister phenomena have focused on how various salts affect the structure of water, and how this perturbation influences various interactions (most notably the hydrophobic effect) [13–16] that stabilize the protein fold. In contrast, until recently, little theoretical analysis has been done on how induced charges in the low-dielectric protein cavity effect the salting-out process.

Recently, using a Kirkwood style analysis coupled with a continuum model description of the electrostatics, Zhou has suggested a theoretical analysis for the salting-out effect, [17] establishing that the work required for salting-out a protein from solution has a quadratic dependence on the square root of the ionic strength. This relationship was used to rationalize the salt dependencies of the stability of cold shock proteins [18] and human FKBP12 protein, [19] demonstrating that salting-out interactions between salts and their induced image charges in the protein cavity significantly contribute to the stability of these proteins under high ionic strength conditions. This work uses this theoretical analysis to investigate this class of interactions by studying the effects of various chlorides on a well characterized protein system ribonuclease t1 (RNAse t1), a system whose spectroscopic and thermodynamic properties are very well understood [20–25]. We have observed that increasing the ionic strength leads to a significant enhancement of the folded state of RNAse t1. The results indicate that although monoprotic chlorides significantly enhance the stability of RNAse t1 at high salt concentrations, these effects cannot always be analyzed meaningfully by applying classical binding models. In contrast, we have shown that for non-interaction ionic species, our measured salt effects on RNAse t1 stability closely follow the trends predicted by salting-out theory, [17] further confirming the theoretical analysis done on cold shock and human FKBP12 proteins [19]. This underlines the importance of considering the effects of point induced image charges on protein stability when salt effects are used to analyze electrostatic contributions to protein structure.

2. Materials and methods

2.1. Materials

Ribonuclease t1 (RNase t1) solution in 2.8 M ammonium sulfate was purchased from Worthington Biochemicals Corporation (Lakewood, NJ). Urea (ultragrade) was purchased from Sigma (St-Louis, MO). All experiments were performed at pH 7.0 in 10 mM bis-tris buffer from Sigma (St-Louis, MO). All salts were purchased from Fisher Scientific (Fair Lawn, NJ). To eliminate the effect of ammonium sulfate on the enzyme RNase t1 storage solution, the enzyme was dialyzed as described previously [23]. To verify the quality of the enzyme, activity measurements were made prior to its use [23], the results were then compared to fresh, non-dialyzed enzyme, which was used as a standard.

2.2. Fluorescence spectroscopy

Steady-state fluorescence spectra were measured on a Fluorolog-3 Horiba Jobin Yvon spectrofluorometer (Edison, NJ). The sample was held in a $10\times4\ mm^2$ quartz cuvette. The data were analyzed with Sigma Plot (Point Richmond, CA) software. All measurements were performed at room temperature in 10 mM bis-tris buffer from Sigma (St-Louis, MO). The samples were excited at 290 nm, the excitation and emission silts were set to a 4 nm bandpass.

2.3. Measurement of protein unfolding free energy

The unfolding free energy was measured by urea denaturation following the technique developed by Pace [25]. In this method a separate series of 1 mL samples, with a final concentration of 0.2 uM RNase t1, was prepared for each predetermined concentration of salt and urea. Every sample was prepared in triplicate for each concentration of urea. The salt concentrations were varied from 50 mM to 1 M. The samples were then left to stand overnight to ensure adequate time for unfolding. The concentration of the stock urea solution was verified by measuring its refractive index on an 115 V AC/DC Refractometer from Fisher Scientific [25].

The extent of denaturation was followed by fluorescence. The parameter characterizing denaturation is the ratio of fluorescence intensities at 330 and 350 nm $\frac{F_{330\ nm}}{F_{350\ nm}}$. This ratio was plotted as a function of urea concentration to yield the unfolding curves. In order to determine the thermodynamic folding parameters we have used the method of Bolen and Santoro [26] fitting the data via non-linear least square minimization using the software Curve Expert (Chattanooga, TN) to Eq. (1):

$$\frac{F_{330\ nm}}{F_{350\ nm}} = y = \frac{y_f + m_f[urea] + (y_u + m_u[urea])\exp\left(-\frac{\Delta G^0_{unfolding} - m[urea]}{RT}\right)}{1 + \exp\left(-\frac{\Delta G^0_{unfolding} - m[urea]}{RT}\right)} \quad (1)$$

where y_f and m_f, y_u and m_u are the slope and intercept of the pre-and post-transition baselines, [*urea*] is the urea concentration, $\Delta G^0_{unfolding}$ standard free energy for protein unfolding in the absence of urea and m is a measure of the dependence of $\Delta G^0_{unfolding}$ on urea concentration, i.e. the cooperativity.

3. Results

3.1. Fluorescence spectroscopy

The fluorescence spectrum of RNAse t1 is sensitive to its structure, and can thus be used to monitor the urea-induced unfolding of the protein. Fig. 1a depicts the fluorescence spectrum of RNAse t1 in the folded (solid line) and urea-induced unfolded state (dashed line). The folded state has an emission peak at 320 nm and as the urea unfolds the protein the emission peak shifts to 350 nm [27]. In order to avoid the effects of the water Raman band which also occurs at 320 nm (when the sample is excited at 290 nm), the unfolding of the protein has been followed by using the ratio of fluorescence intensities measured at 330 nm (F_{330}) and 350 nm (F_{350}). Monitoring the fluorescence changes between these two wavelengths has been successfully used by several to characterize the unfolding of RNAse t1 [21,24,25,28–35]. The addition of salts has no effect on the fluorescence spectrum of folded RNAse t1, with the exception of $ZnCl_2$ which is the only salt that quenches the fluorescence of the protein (Fig. 1b), this quenching follows a hyperbolic binding profile (Fig. 1b, inset).

3.2. The unfolding of RNAse t1 at low ionic strength

The unfolding of RNAse t1 can be monitored by recording the ratio $\frac{F_{330}}{F_{350}}$. Fig. 2 plots the changes in the $\frac{F_{330}}{F_{350}}$ ratio of RNAse t1 as a function of denaturant concentration in order to obtain the unfolding curve of RNase t1 in pH 7 buffer at low ionic strength. The data demonstrate that this ratio changes from ~1.5 for the folded state to ~0.7 for the unfolded state. Because the unfolding of RNAse t1 has been shown to closely approach a two-state mechanism, [24,25] the free energy of RNAse t1 unfolding ($\Delta G^0_{unfolding}$) can be easily obtained from the unfolding data in Fig. 2 by using Eq. (1). The data are well correlated

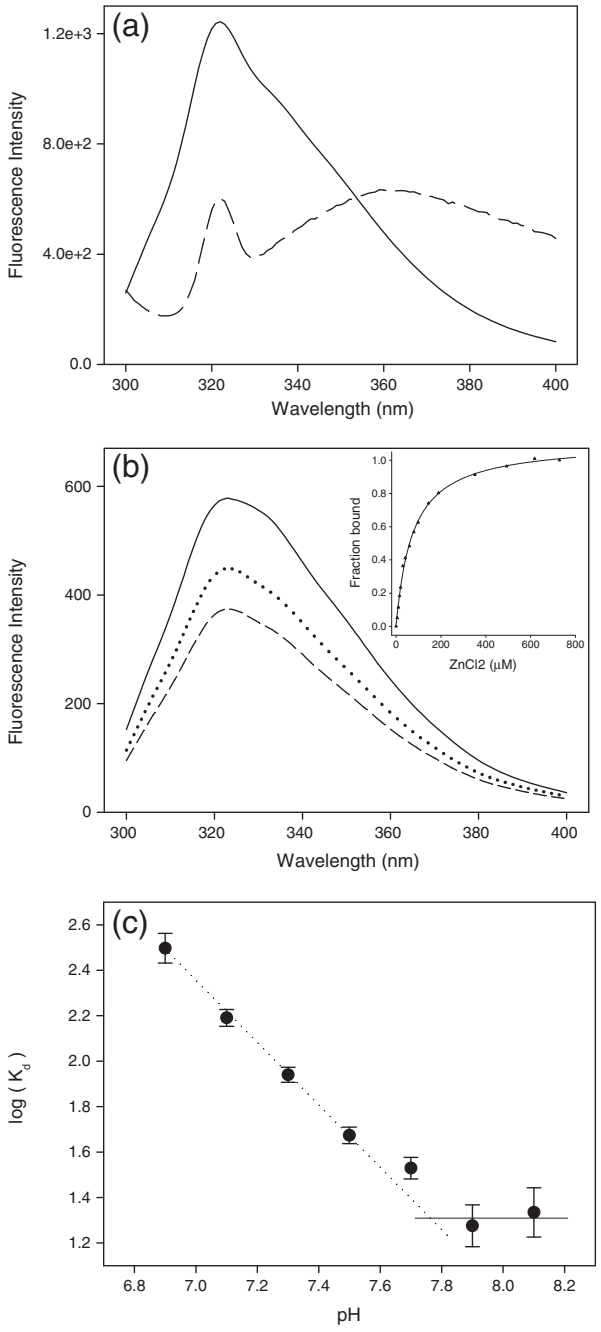

Fig. 1. a) The fluorescence spectrum of RNAse t1 in the folded state (solid line) and in the unfolded state (dashed line), showing the Raman peak; b) the fluorescence spectrum of RNAse t1 in the folded state and absence of $ZnCl_2$ (solid line), in the presence of 50 μM $ZnCl_2$ (dashed line), in the presence of 50 μM $ZnCl_2$ and 100 mM $MgCl_2$ (dotted line), the inset fits the zinc chloride quenching data to a hyperpolic binding curve (we have corrected for the Raman peak); c) the pH dependence of the dissociation constant K_d of the Zn^{2+} ligand in micromolar units, $\log(K_d) = 6\text{-}\log(K_b)$. All measurements were performed at room temperature in 10 mM bis-tris buffer, the pH in 1a and 1b is set to 7.7. The samples were excited at 290 nm, the excitation and emission silts were set to a 4 nm bandpass. The concentration of protein is always 0.5 μM.

(coefficient of determination, $R^2 > 0.999$). This fit yields the following parameter values and their defined uncertainties: $\frac{\Delta G^0_{unfolding}}{RT} = 10.01 \pm 0.01$; $\frac{m}{RT} = 2.012 \pm 0.001$ and $[urea]_{1/2=5.10\pm0.05\ M}$, where $[urea]_{1/2}$ is the midpoint concentration of the unfolding curve. It must be emphasized that because these unfolding experiments are done on samples that are prepared and left to stand for 12 h, issues of sample variation and reproducibility become important. In order to check for reversibility,

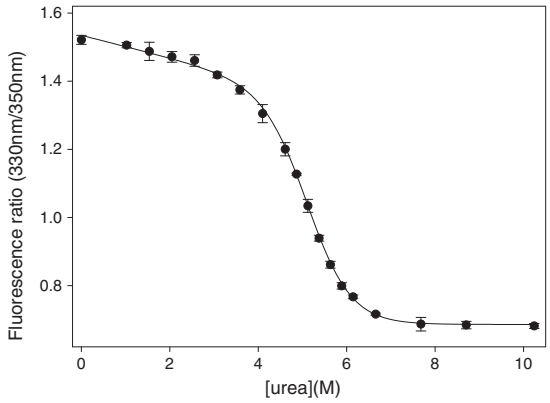

Fig. 2. The unfolding profile of RNAse t1 dissolved in pH 7 10 mM tris buffer at low ionic strength. The plot is obtained from plotting the parameter $\frac{F_{330}}{F_{350}}$ (as defined in the text) as a function of urea concentration. The correlation line is the best fit to Eq. (1).

multiple (about 20) measurements of the unfolding of RNase t1 in pH 7 buffer at low ionic strength have been performed. All these results are extremely well correlated with Eq. (1) and the following mean values for Eq. (1) parameters for RNAse t1 in pH 7 buffer at low ionic strength are obtained accompanied by their standard deviations: $\frac{\Delta G^0_{unfolding}}{RT} = 9.6 \pm 0.5$; $\frac{m}{RT} = 2.9 \pm 0.1$ and $[urea]_{1/2=5.2\pm0.3\ M}$. These values are consistent with the literature values [36,37].

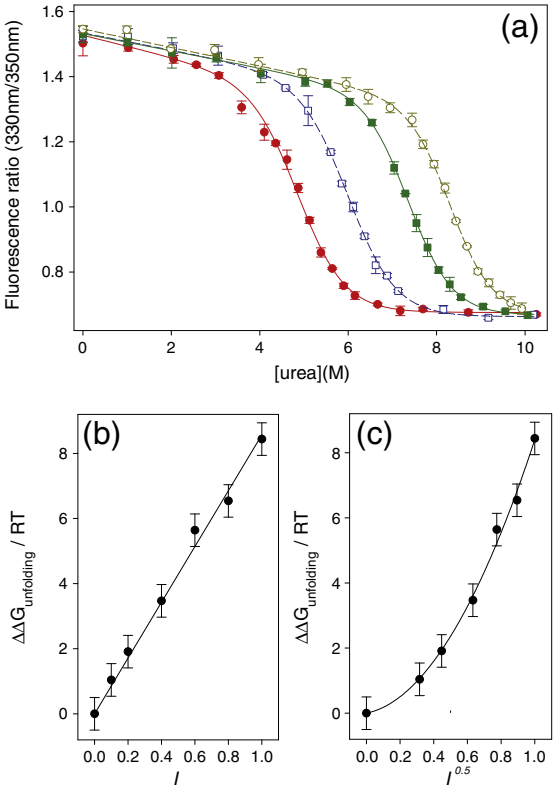

Fig. 3. a) Unfolding profiles for RNAse t1 in various NaCl solutions, the pH of all solutions are maintained at 7 using 10 mM tris buffer; b) the dependence of $\frac{\Delta\Delta G^0_{unfolding}}{RT}$ on ionic strength for various NaCl solutions, the solid line is the fit obtained to Eq. (2); c) b) the dependence of $\frac{\Delta\Delta G^0_{unfolding}}{RT}$ on the square root of the ionic strength for various NaCl solutions, the solid line is the fit obtained to Eq. (4).

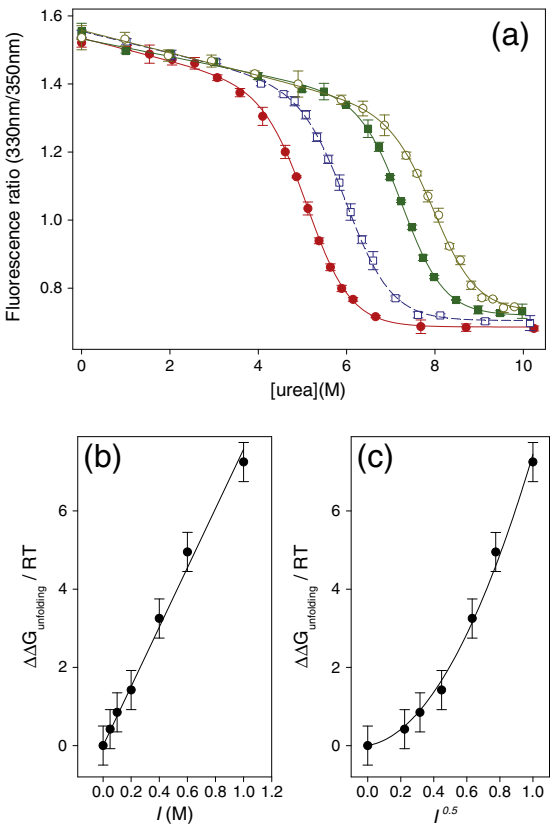

Fig. 4. a) Unfolding profiles for RNAse t1 in various KCl solutions, the pH of all solutions are maintained at 7 using 10 mM tris buffer; b) the dependence of $\frac{\Delta\Delta G^0_{unfolding}}{RT}$ on ionic strength for various KCl solutions, the solid line is the fit obtained to Eq. (2); c) b) the dependence of $\frac{\Delta\Delta G^0_{unfolding}}{RT}$ on the square root of the ionic strength for various KCl solutions, the solid line is the fit obtained to Eq. (4).

3.3. The effect of the monoprotic chlorides on the unfolding of RNAse t1

Figs. 3a, 4a and 5a show the effects of the monoprotic salts NaCl, KCl and LiCl on the unfolding profile of RNAse t1 as defined by the ratio $\frac{E_{330\ nm}}{F_{350\ nm}}$. The addition of these salts significantly influences the stability of the protein. All data have been fitted to Eq. (1) and the values of R^2, $\frac{\Delta G^0_{unfolding}}{RT}$ and $\frac{m}{RT}$ have been tabulated in Table 1 for the different monoprotic salt species at various concentrations. In addition the values of $\left(\frac{\Delta\Delta G^0_{unfolding}}{RT}\right) = \frac{\Delta G^0_{unfolding}}{RT} - (9.6 \pm 0.5)$ — i.e. the salt contributions to the standard unfolding free energy — are also given in this table. In reporting $\left(\frac{\Delta\Delta G^0_{unfolding}}{RT}\right)$ values, its associated error of reproducibility has also been propagated as pointed out earlier.

Figs. 3b and 4b and 5b depict the dependence of $\left(\frac{\Delta\Delta G^0_{unfolding}}{RT}\right)$ values on the ionic strength (I). Often the free energy of folding is correlated linearly with the ionic strength [38–40]. The solid line in these figures is the best fit to the equation:

$$\left(\frac{\Delta\Delta G^0_{unfolding}}{RT}\right) = a * I \qquad (2)$$

The results of this linear correlation are listed in Table 3. The values of $\left(\frac{\Delta\Delta G^0_{unfolding}}{RT}\right)$ for NaCl and KCl are well correlated linearly, while the LiCl data show larger scatter. Because in monoprotic salts the numerical values of the ionic strength and salt concentration

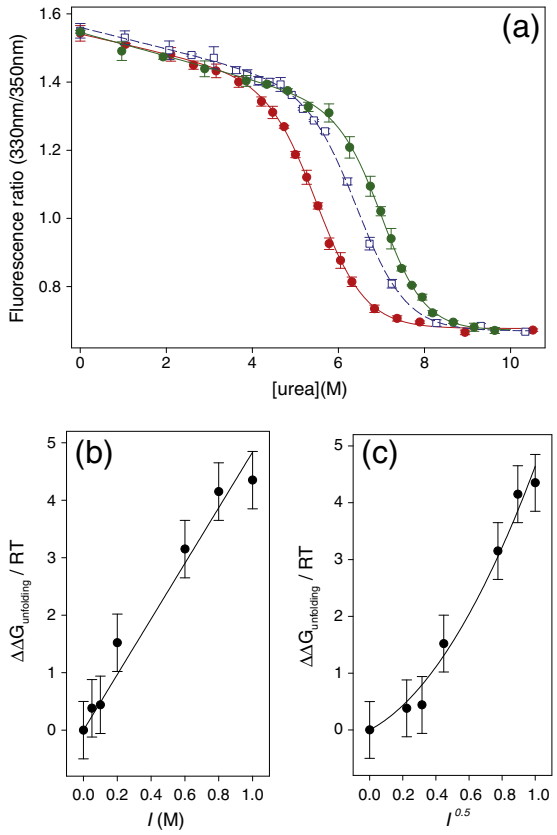

Fig. 5. a) Unfolding profiles for RNAse t1 in various LiCl solutions, the pH of all solutions are maintained at 7 using 10 mM tris buffer; b) the dependence of $\frac{\Delta\Delta G^0_{unfolding}}{RT}$ on ionic strength for various LiCl solutions, the solid line is the fit obtained to Eq. (2); c) b) the dependence of $\frac{\Delta\Delta G^0_{unfolding}}{RT}$ on the square root of the ionic strength for various LiCl solutions, the solid line is the fit obtained to Eq. (4).

are equal, the depiction in Figs. 3b and 4b and 5b can also be used to investigate the applicability of binding models to this salt-induced increase in protein stability. If a ligand selectively binds to the folded form of a protein, an increase in ligand concentration stabilizes the protein folded state via the following equation: [34]

$$\left(\frac{\Delta\Delta G^0_{unfolding}}{RT}\right) = \Delta n \ln(1 + K * [ligand]) \quad (3)$$

where in this equation Δn is the number of ligand binding sites on the protein and K is the average binding constant of each site. If it is assumed that the salt cations are binding ligands, the data can be analyzed using Eq. (3). The results for this fit are shown in Table 4. The data are indeed correlated with this equation; however, as shown in the Discussion section, interpreting our results on the basis of Eq. (3) is problematic.

Table 1
The effect of monoprotic salts on the unfolding profile of RNAse t1; all parameters are defined in the text.

	$\frac{\Delta G^0_{unfolding}}{RT}$	$\frac{m}{RT}$	R^2	$\frac{\Delta\Delta G^0_{unfolding}}{RT}$
[NaCl] (M)				
0.1	10.64 ± 0.01	1.882 ± 0.002	0.999	1.0 ± 0.5
0.2	11.51 ± 0.02	1.851 ± 0.003	0.998	1.9 ± 0.5
0.4	13.07 ± 0.01	1.862 ± 0.001	0.999	3.5 ± 0.5
0.6	15.24 ± 0.03	2.014 ± 0.004	0.998	5.6 ± 0.5
0.8	16.14 ± 0.02	1.991 ± 0.002	0.997	6.5 ± 0.5
1.0	18.04 ± 0.01	2.121 ± 0.001	0.999	8.4 ± 0.5
[KCl] (M)				
0.05	10.02 ± 0.01	2.010 ± 0.001	0.999	0.4 ± 0.5
0.1	10.45 ± 0.02	2.012 ± 0.003	0.999	0.9 ± 0.5
0.2	11.02 ± 0.01	1.946 ± 0.001	0.999	1.4 ± 0.5
0.4	12.85 ± 0.03	1.861 ± 0.004	0.999	3.3 ± 0.5
0.6	14.55 ± 0.02	2.102 ± 0.001	0.999	5.0 ± 0.5
1.0	16.85 ± 0.02	2.031 ± 0.002	0.999	7.3 ± 0.5
[LiCl] (M)				
0.05	9.98 ± 0.01	1.734 ± 0.002	0.999	0.4 ± 0.5
0.1	10.04 ± 0.01	1.701 ± 0.003	0.998	0.5 ± 0.5
0.2	11.12 ± 0.04	1.737 ± 0.001	0.996	1.5 ± 0.5
0.6	12.75 ± 0.01	1.830 ± 0.004	0.995	3.2 ± 0.5
0.8	13.75 ± 0.03	1.962 ± 0.002	0.997	4.2 ± 0.5
1.0	13.95 ± 0.02	1.993 ± 0.005	0.996	4.9 ± 0.5

Table 2
The effect of diprotic salts on the unfolding profile of RNAse t1; all parameters are defined in the text.

	$\frac{\Delta G^0_{unfolding}}{RT}$	$\frac{m}{RT}$	R^2	$\frac{\Delta\Delta G^0_{unfolding}}{RT}$
[$MgCl_2$] (M)				
0.05	11.90 ± 0.01	2.071 ± 0.002	0.996	2.3 ± 0.5
0.2	14.02 ± 0.03	1.923 ± 0.003	0.998	4.4 ± 0.5
0.4	16.04 ± 0.01	2.042 ± 0.001	0.999	6.4 ± 0.5
0.8	18.60 ± 0.03	1.926 ± 0.004	0.999	9.0 ± 0.5
1.0	19.92 ± 0.01	2.023 ± 0.001	0.997	10.3 ± 0.5
[$ZnCl_2$] (M)				
0.0001	10.02 ± 0.01	2.010 ± 0.001	0.999	0.4 ± 0.5
0.0002	10.45 ± 0.02	2.012 ± 0.003	0.999	0.9 ± 0.5
0.0004	11.02 ± 0.01	1.946 ± 0.001	0.999	1.4 ± 0.5
0.0006	12.85 ± 0.03	1.861 ± 0.004	0.999	3.3 ± 0.5

Table 3
Parameters obtained from fitting the data in Tables 1 and 2 to Eq. (2).

Salt	A	R^2
NaCl	8.5 ± 0.1	0.992
KCl	7.5 ± 0.1	0.992
LiCl	4.8 ± 0.2	0.966
$MgCl_2$	3.8 ± 0.4	0.844

3.4. The effect of $ZnCl_2$ on the unfolding of RNAse t1

It is well known that zinc ions specifically interact with RNAse t1 and inhibit catalysis through a pH dependent mixed mechanism at micromolar concentrations [41,42]. The binding of zinc ions quenches RNAse t1 fluorescence (Fig. 1b). The addition of zinc quenches the fluorescence but does not change the shape of the protein fluorescence spectrum, indicating that it is unlikely that the metal causes a great structural perturbation. The zinc quenching profile follows a simple ligand binding profile (Fig. 1b inset), with a binding constant of 29,000 ± 2000 M^{-1} at room temperature at pH 7.7. This value is close to the enzyme binding constants determined via inhibition assays. The quenching most likely occurs via an electron-transfer mechanism because: a) there is no spectral overlap between the absorbance on $ZnCl_2$ and the protein fluorescence, thereby ruling out FRET; b) zinc has an ionization potential of ~9.39 eV [43] and therefore can accept an electron from an excited tryptophan that has an ionization potential of ~7.8 eV [44].

In our studies of zinc ion binding, the data show strong temperature dependence. Between 5 and 40 °C, the binding constant K_b at pH 7 follows linear Van't Hoff behavior expressed by the linear equation "$\ln K_b = -(13000 \pm 2000) * \frac{1}{T} + (35 \pm 4)$". We only observe this strong temperature dependence in zinc ion binding, indicating a strong enthalpic contribution to binding. The binding constants also exhibit

Table 4
Parameters obtained from fitting the data in Tables 1 and 2 to Eq. (3).

Salt	ΔN	$K\ (M^{-1})$	R^2
NaCl	12 ± 3	0.2 ± 0.1	0.995
KCl	9 ± 3	0.4 ± 0.1	0.997
LiCl	1.8 ± 0.3	1.9 ± 0.4	0.990
$MgCl_2$	1.9 ± 0.2	10 ± 2	0.992
$ZnCl_2$	Set to 1	6000 ± 200	0.980

strong pH dependence. This pH dependence is shown in Fig. 1c. The data from Fig. 1c demonstrates that the binding of zinc involves a moiety having a pK_a close to 7.7; this is far removed from the pK_a values of surface carboxylates (less than 4).[1] Therefore, because RNAse t1 lacks free cysteines, we suggest that it may be likely that histidine residues are involved in the zinc binding process.

The effect of $ZnCl_2$ on the RNAse t1 folding profile is shown in Fig. 6a. The addition of zinc increases stability of RNAse t1. The amounts of $ZnCl_2$ added are less than 1 mM; such low salt concentrations cannot electrostatically affect the protein, therefore, the observed increase in stability is not due to electrostatic or salting-out effects, but rather is a consequence of zinc ion binding. The unfolding data are fitted to Eq. (1) and have tabulated values of R^2, $\frac{\Delta G^0_{unfolding}}{RT}$, $\left(\frac{\Delta\Delta G^0_{unfolding}}{RT}\right)$ and $\frac{m}{RT}$ in Table 2. The values of $\frac{\Delta\Delta G^0_{unfolding}}{RT}$ as a function of $ZnCl_2$ concentration are plotted in Fig. 6b. The data are fitted to Eq. (3), with only one binding site yielding a binding constant $K = 6000 \pm 200\ (M^{-1})$ for zinc ion that is very close to the results in Fig. 1c (fitting parameters to Eq. (3) are given in Table 4). In all measurements the concentrations of zinc ion have been kept below the solubility limit of zinc hydroxide.

3.5. The effect of $MgCl_2$ on the unfolding of RNAse t1

Fig. 7 demonstrates the effect of $MgCl_2$ on the unfolding profile of RNAse t1. $MgCl_2$ salts significantly influence the stability of the protein. All data are fitted to Eq. (1) and the values of R^2, $\frac{\Delta G^0_{unfolding}}{RT}$, $\left(\frac{\Delta\Delta G^0_{unfolding}}{RT}\right)$ and $\frac{m}{RT}$ are given in Table 1b. The effect of $MgCl_2$ on the fluorescence spectrum of RNAse t1 has also been investigated in this work. As it can be observed in Fig. 1b, the addition of 100 mM $MgCl_2$ to a solution of RNAse t1 that contains 50 μM $ZnCl_2$ leads to a 30% recovery of protein fluorescence. The addition of none of the monoprotic salts causes such a recovery of fluorescence. Because the species Mg^{+2} cannot receive an electron from excited tryptophan, it is likely that this fluorescence recovery is caused by the magnesium ions replacing some of the zinc quenchers. This demonstrates that Mg^{2+} ions behave similarly to Zn^{+2} and also specifically bind RNAse t1. This is confirmed by fitting the $\left(\frac{\Delta\Delta G^0_{unfolding}}{RT}\right)$ data to the classical ligand binding model. Fig. 8 plots $\left(\frac{\Delta\Delta G^0_{unfolding}}{RT}\right)$ as function of $MgCl_2$ concentration. The data show reasonable ($R^2 > 0.992$) correlation with Eq. (3) and the results of this fit are shown in Table 4 , from this a binding constant of approximately 10 M^{-1} is obtained for the magnesium ion.

[1] One potential complication in interpreting this data is that the prevalent form of zinc ion in solution $[Zn(H_20)_6]^{2+}$ may participate in the equilibrium $[Zn(H_20)_6]^{2+} \rightleftarrows [Zn(H_20)_5OH]^{+} + H^{+}$ that has a $pK_a \approx 9$ [56]. This may complicate the interpretation, but does not strengthen the case for the participation of carboxylates. If carboxylates are involved in zing binding they must replace one of the ligands of zinc. Water is the most labile ligand, however the cost of replacing one of the waters of $[Zn(H_20)_5OH]^{+}$ with carboxylate is much more than that of $[Zn(H_20)_6]^{2+}$, because the carboxylates must overcome repulsion from the hydroxyl groups. Therefore, if carboxylates are involved, one would expect to see an *increase* in binding as the pH is lowered, which is the opposite of what we observe.

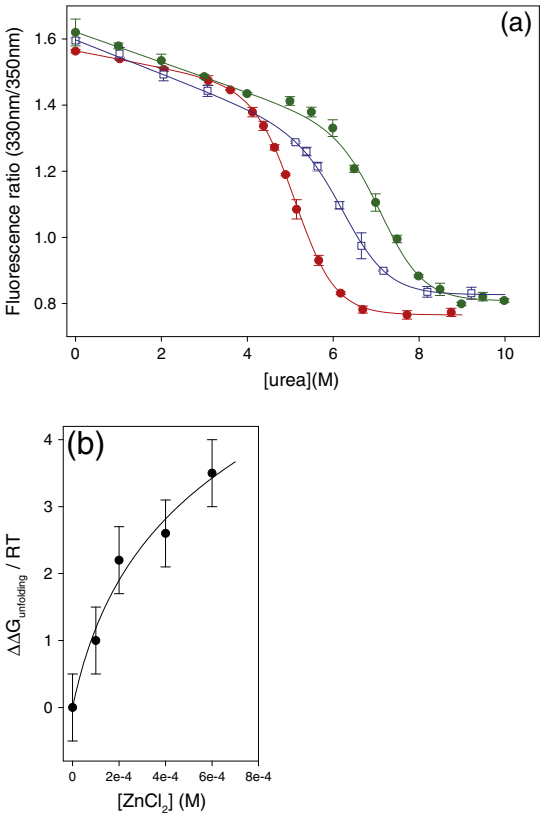

Fig. 6. a) Unfolding profiles for RNAse t1 in various $ZnCl_2$ solutions, the pH of all solutions are maintained at 7 using 10 mM tris buffer; b) the dependence of $\frac{\Delta\Delta G^0_{unfolding}}{RT}$ on $ZnCl_2$ concentration, the solid line is the fit obtained to Eq. (3).

4. Discussion

The data demonstrate that the addition of monoprotic chlorides, NaCl, KCl and LiCl to the protein solvent stabilizes the folded form of RNAse t1. Based on the crystal structure of Saenger [21,45], it has been suggested that the cations bind to surface carboxylates, with the carboxylate replacing one of the coordinating ions of the cations. Although traditionally cation binding has been invoked to explain this additional stability [21,36,45], the results of this work tend to argue against this interpretation. First, in the case of sodium and potassium, the binding constants are extremely small and the total number of binding sites is rather large; while lithium has only two binding sites with a somewhat larger binding constant. Therefore, a paradox

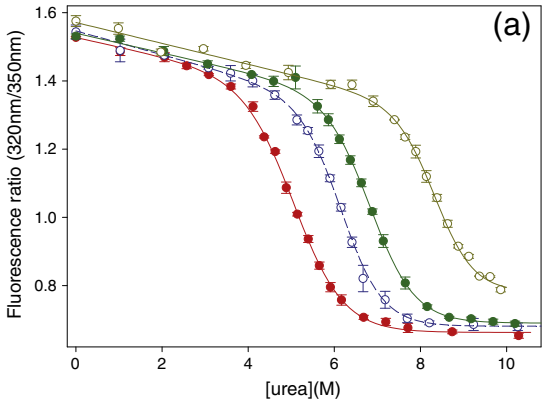

Fig. 7. a) Unfolding profiles for RNAse t1 in various $MgCl_2$ solutions, the pH of all solutions are maintained at 7 using 10 mM tris buffer.

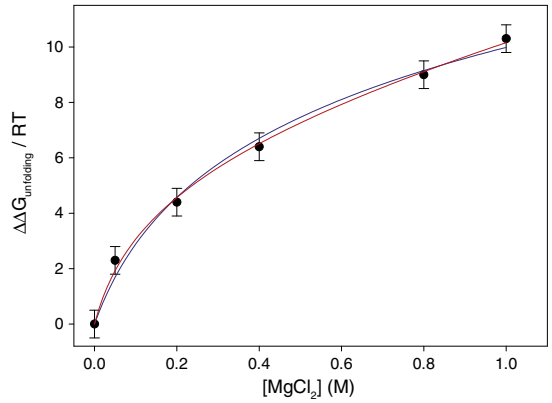

Fig. 8. Fitting the values of $\frac{\Delta\Delta G^0_{unfolding}}{RT}$ for RNAse t1 as a function of $MgCl_2$ concentration to Eq. (3) (blue line) and Eq. (15) (red line).

seems to exist: namely, that the weaker interacting the ion is, it interacts with a larger number of sites. Secondly, the pH-dependent studies of Zn^{2+} binding indicate the low probability of carboxylate involvement in cation binding for zinc and magnesium ions, and perhaps other cations.[2] If, on the other hand, we simplify Eq. (3) by applying the linear approximation at small K we obtain:

$$\left(\frac{\Delta\Delta G^0_{unfolding}}{RT}\right) = \Delta n \ln(1 + K * [ligand]) \approx \Delta n * K * [ligand] \quad (3a)$$

which is equivalent to the linear relationship of Eq. (2), the slope of the equation being equal to $\Delta n * K$; this kind of a linear relationship with the ionic strength is often seen in salt studies of proteins [38–40,46]. The values of $\Delta n * K$ would therefore be equal to parameter (a) of Table 2 and our measured values of a follow the order $a_{NaCl} > a_{KCl} > a_{LiCl}$. In the case where the value of Δn is taken to be equal for all monoprotic salts, the values of K will follow: $K_{NaCl} > K_{KCl} > K_{LiCl}$; these values seem more reasonable, because it is less likely that the number of surface sites available for the small penetrable lithium ion is significantly less than sodium — in fact, a reasonable fit ($R^2 > 0.97$) is also obtained if the LiCl data is fitted to the classical binding equation and the Δn is constrained to be larger than 7. If the Δn is considered to be 10 (the average of sodium and potassium), the values of K for all monoprotic salts would be smaller than 1 M^{-1}. When the values of K are this low it is more appropriate to consider them as solvent exchange constants as opposed to binding constants [47,48]. Applying classical binding models to these cases often lead to non physical results, and the enhanced protein stability that we observe is the result of salt exchanging with the water molecules of the protein hydration sphere as opposed to any specific salt protein interaction [49].

As it has been pointed out in the Introduction, the placing of a point charge in the near vicinity of the low-dielectric protein cavity will lead to increased salting-out effects. However, this exchange process is also accompanied by an increase in the ionic strength of the solvent. We can now discuss the involvement of salting-in and salting-out interactions in the stabilization of the folded form of RNAse t1. In the absence of any specific interactions, the salt contribution to the standard unfolding free energy $\left(\frac{\Delta\Delta G^0_{unfolding}}{RT}\right)$ can be broken down to the following components:

$$\left(\frac{\Delta\Delta G^0_{unfolding}}{RT}\right) = (salting{-}out \quad folded) + (salting{-}out \quad unfolded) + (salting{-}in \quad folded) + (salting{-}in \quad unfolded) \quad (5)$$

The salting-in contributions of Eq. (5) is due to Debye–Hückel type interactions [17,19,50,51]. These interactions have two aspects: First, each charged residue induces a counterion cloud in the solvent and therefore has a stabilizing interaction with the salt ions (charged residue solvation by salts); secondly, salts can weaken interactions between charged residues (charge screening by salts). The first aspect can be analyzed using the generalized Born model [51], the solvation energy of a charged group has the form:

$$\frac{Aq^2}{r}\left(1 - \frac{e^{-\kappa r}}{\varepsilon_s}\right) \cdot f \quad (6)$$

where A is a unit dependent constant, q is the magnitude of the charge, ε_s is the dielectric constant of the solvent, r is the Born radius of the charge group, $\kappa = 0.3\sqrt{I}$ is the Debye screening parameter (I is the ionic strength) and f is the fraction of the area of the charged group that is solvent accessible. In the unfolded state the charges are more accessible to solvent and the increase in solvent accessibility coupled to an increase in the local dielectric constant experienced by the charge would cause the induced solvent counterion cloud to stabilize the unfolded state more than the folded state [19], causing a reduction of the magnitude of $\left(\frac{\Delta\Delta G^0_{unfolding}}{RT}\right)$ and will reduce thus reduce the stability of the folded state relative to the unfolded state.

In contrast, the second aspect of salting-in, i.e. the interactions between two charged groups will have the form:

$$B\frac{q_1 q_2}{d}\left(1 - \frac{e^{-\kappa d}}{\varepsilon_s}\right) \quad (7)$$

where B is a unit dependent constant, q_1 and q_2 are the magnitude of each charge, κ is the Debye screening parameter, d is the distance between the charges and ε_s is the dielectric constant of the solvent. Because the distances between charges are much less in the folded state than in the unfolded state charge-charge interactions will be much stronger in the folded state, and salts will have a larger screening effect on these interactions in the folded state [19]. RNAse t1 has a large number of charged residues (~16) and 12 of these residues are negatively charged. The overall charge of the protein is negative and repulsion is the dominant charge–charge interaction in the folded state of this protein. The introduction of salt can screen these repulsive interactions in the folded state, causing an increase in the magnitude of $\left(\frac{\Delta\Delta G^0_{unfolding}}{RT}\right)$, thereby enhancing the stability of the folded state relative to the unfolded state. Therefore, the net salting-in effect on highly charged proteins $\{(salting-in \quad folded) + (salting-in \quad unfolded)\}$ is a sum of interactions that stabilize both

Table 5
Parameters obtained from fitting the data in Table 1 to Eq. (10-a).

Salt	B	C	R^2
NaCl	1.0 ± 0.3	7.3 ± 0.4	0.995
KCl	0.7 ± 0.3	6.7 ± 0.3	0.994
LiCl	1.5 ± 0.4	3.1 ± 0.4	0.982

[2] We may suggest that the crystallographic data suggesting that the coordination of Zinc is via a surface Asp15 carboxylate and to six water molecules forming a dodecahedron of square anti-prismatic form [36,45] in inapplicable to this work. The reason for this is that Saenger obtained his crystals at pH 5, in which according to Fig. 6 and enzyme inhibition studies, zinc binding is at a minimum (crystals can not be collected at neutral pH because zinc ion precipitates out as zinc hydroxide at millimolar concentrations).

the folded and unfolded forms to almost the same extent in opposite directions. This contribution is clearly ionic strength dependent:

$$\{(salting{-}in\ \ folded)+(salting{-}in\quad unfolded)\}=F\left(\sqrt{I}\right)\approx\alpha\sqrt{I}+\beta I+\ldots. \tag{8}$$

The function$F\left(\sqrt{I}\right)$ depends on ionic strength. Because $F\left(\sqrt{I}\right)$ is significantly smaller than either of the component $\left(\frac{\Delta\Delta G^0_{unfolding}}{RT}\right)$terms, we can expand it as a polynomial in *I*. What must be emphasized is that in the derivation above none of the coefficients of Eq. (8) are dependent on the nature of the salt and the salting-in interactions only depend on the ionic strength.

In the case of salting-out interactions, because the salt accessible surface area of the unfolded state is much larger than that of the folded state, it can be assumed that the magnitude of (*salting-out folded*) is much smaller than that of(*salting-out unfolded*). Theoretical calculations [17] suggest that (*salting-out unfolded*) follows the form:

$$(salting{-}out\ \ unfolded)=b*\sqrt{I}+c*I \tag{9}$$

The parameter *b* is dependent on the "exclusion diameter" of the monoprotic salts and decreases while the exclusion diameter increases, while *c* is not size-dependent [17]. Therefore, the total salt contribution to the standard unfolding free energy can be expressed as:

$$\left(\frac{\Delta\Delta G^0_{unfolding}}{RT}\right)=b\sqrt{I}+cI+\left(\alpha\sqrt{I}+\beta I+\ldots\right) \tag{10}$$

In Figs. 3c, 4c and 5c the dependence of $\left(\frac{\Delta\Delta G^0_{unfolding}}{RT}\right)$ on the square root of the ionic strength is shown. The data are fitted to a quadratic of the form:

$$\left(\frac{\Delta\Delta G^0_{unfolding}}{RT}\right)=b'*\sqrt{I}+c'*I \tag{10 - a}$$

where *I* is the ionic strength and *b*' and *c*' are constants. The lines in Figs. 3c, 4c and 5c are obtained by fitting the data to Eq. (4) and the results are shown in Table 5. All $\left(\frac{\Delta\Delta G^0_{unfolding}}{RT}\right)$ data are well expressed by a quadratic equation in $\sqrt{I}$ indicating that the contribution of higher terms in Eq. (8) is most likely negligible. According to Eq. (10) the experimentally determined coefficient *b*'is a sum of *b* (from salting-out) and α (from salting-in). The parameter *b* decreases as the salt exclusion diameter increases [17] while α is solely a function of ionic strength and is not dependent on salt type. In the continuum model the salt exclusion diameter d_{ex}, has been taken to be ~1.25 *d*, [17] where *d* is the Pauling diameter of the salt [52]. This trend is indeed observed in the monoprotic data where the trend in *b*':

$$b'_{KCl}(0.7)<b'_{NaCl}(1.0)<b'_{LiCl}(1.5) \tag{11a}$$

Follows the opposite trend in d_{ex}:

$$d_{exLiCl}(3.18\,\text{Å})<d_{exNaCl}(3.52\,\text{Å})<d_{exKCl}(3.98\,\text{Å}) \tag{11b}$$

The fact that this trend is observed indicates that the interaction between the ions in the near vicinity of the protein and their mirror induced charges in the protein medium is a significant contributor to the observed salt-induced stability of the protein.

For a series of monoprotic chlorides, the theoretical model predicts that *c* must not significantly change with the nature of the salt, while our derivation earlier indicates that β like α should only depend on ionic strength. However, the experimental parameter*c*' follows the following trend:

$$c'_{\mathrm{NaCl}}\,(7.3)\approx c'_{\mathrm{KCl}}\,(6.7)>c'_{\mathrm{LiCl}}(3.1) \tag{12}$$

This trend is different from the prediction of theory [17] and the values of *c*'are not constant. On the other hand, this trend follows the Hofmeister series (i.e. NaCl stabilizes proteins more or less equal to KCl and more than LiCl). Because the effect described by the theoretical model [17] is only the effect of point charges, any differences observed in the *c*' values are likely due to salt specific effects. These effects are still weak and are therefore still due to salt exchanging for solvent water molecules in the hydration shell. Because the chloride is the common ion in all three salts, these differences must be to a large part due to the nature of the cation.

What distinguishes lithium from the other two cations is that it has been shown that it can participate in a variety of weak interactions with various segments of the protein. For example, lithium ions have been shown to weakly interact with the amide bond of the polypeptides [53] and with hydrophobic groups [54] and thus help solubilize these moieties. These weak interactions are not localized to specific protein locations and are of the same magnitude of the interaction of water molecules with the amide bond. Conceptually, this property of Li^+ may be considered to be similar to that of urea: urea has also been shown to weakly interact with amide bonds [55] but these interactions cannot considered to be site specific, but are rather thought to be a sum of a large number of weak interactions spreading the whole hydration surface of the protein. Thus, when LiCl replaces solvent water in the protein hydration sphere, two competing weak interactions are affecting the stability of the protein folded state: the stabilizing effect of salting-out interactions and the destabilizing effect of solubilizing amide bonds and hydrophobic moieties. This can be represented as:

$$\left(\frac{\Delta\Delta G^0_{unfolding}}{RT}\right)_{\mathrm{LiCl}}=\left(\frac{\Delta\Delta G^0_{unfolding}}{RT}\right)_{electrostatic}+\left(\frac{\Delta\Delta G^0_{unfolding}}{RT}\right)_{\mathrm{solubilization}} \tag{13}$$

This can be re-written as:

$$\left(\frac{\Delta\Delta G^0_{unfolding}}{RT}\right)=b'*\sqrt{I}+c'*I+\left(\frac{\Delta\Delta G^0_{unfolding}}{RT}\right)_{\mathrm{solubilization}} \tag{13a}$$

The contribution of $\left(\frac{\Delta\Delta G^0_{unfolding}}{RT}\right)_{\mathrm{solubilization}}$ is destabilization and decreases the magnitude of $\left(\frac{\Delta\Delta G^0_{unfolding}}{RT}\right)$ as the concentration of LiCl increases. At low LiCl concentrations, this parameter can be assumed to be linearly dependent on salt concentration $\left(\frac{\Delta\Delta G^0_{unfolding}}{RT}\right)_{\mathrm{solubilization}}=-\sigma*I$ yielding:

$$\left(\frac{\Delta\Delta G^0_{unfolding}}{RT}\right)=b'*\sqrt{I}+(c'{-}\sigma)*I \tag{13b}$$

Thereby, providing an explanation for the observed inequality expressed in Eq. (12).

Interpreting the effects of the divalent salts on RNAse t1 stability is simpler. The $ZnCl_2$ salt data follow the classical binding model in a straightforward fashion. In the case of $MgCl_2$, the binding model results in the following fit:

$$\left(\frac{\Delta\Delta G^0_{unfolding}}{RT}\right)=1.9*\ln(1+10c) \tag{14}$$

This implies that RNAse t1 has two binding sites with an average binding constant of 10 M^{-1}. However, the binding model does not consider the consequences that exchanging one formal unit of $MgCl_2$ with one molecule of water may have on the thermodynamics of the folded state of the protein. The presence of a small highly charged ion like

Mg^{2+} ion in the near vicinity of the protein will definitely stabilize the folded state via salting-out interactions, while solubilizing interactions similar to that of Li^{2+} may cause the folded state to become less stable.

Because the theoretical model described earlier has been derived using the Poisson-Boltzmann distribution, it may not be appropriate to apply this model to a multivalent high-charge-density system like $MgCl_2$. However, the effects of point image charges or solubilizing interactions are still the result of a summation over a large number of weak interactions. Therefore, in the case of low salt concentrations we can modify Eq. (14) to:

$$\left(\frac{\Delta\Delta G^0_{unfolding}}{RT}\right) = \Delta n * \ln(1 + Kc) + \phi * c \tag{15}$$

where the first term is the contribution of binding and the second term is a linear term that approximates the effects of exchanging $MgCl_2$ for water molecules in the solvent shell. If the binding site is limited to one, the values of $K = 24 \pm 1$ (M^{-1}), $\phi = 2.7 \pm 0.3$ are obtained from a fit having an $R^2 = 0.997$, which results in as good a fit as before (Fig. 8), without the necessity to postulate any additional binding sites than the zinc binding site. Therefore, it is very likely that $MgCl_2$ stabilizes the protein both through binding and through salting-out interactions.

5. Conclusions

This work has investigated the hypothesis that a major contributor to the salt-induced stability of RNAse t1 folded state is the interaction between ions located near in the protein–water interface and their point image charges located in the low-dielectric protein cavity. The analyzed data for monoprotic salts is consistent with following predictions of theoretical models that relate salting-out interactions with protein stability: first, the salt effects on RNAse t1 manifest themselves via exhibiting a quadratic dependence of the folding free energy on the square root of the ionic strength; second, because RNAse t1 is highly charged, this quadratic stabilization has manifested itself in only positive coefficients; third, the stabilization free energy does follow the dependence on salt exclusion diameter as predicted by theory.

As a control, binding models have also been considered for analyzing the results of this work. In the case of ZnCl that contains a tightly binding metal ion, classical binding models adequately describe the enhanced stability. In contrast, applying classical binding models to monoprotic salt thermodynamic data yield binding constants that are so small that they ought to be considered as solvent exchange constants. In these cases it is difficult to define binding sites in a classical sense, therefore the application of classical binding models in these cases lead to non-realistic results. The weakly interacting salt $MgCl_2$ presents a special case in which both binding and salting-out contribute to the observed stability.

It must also be emphasized that "goodness of fit" is not the criterion used for discarding the classical binding model for monoprotic salts. If anything, from a statistical standpoint, Eq. (3) gives an equivalent or somewhat better-correlated fit to the data in this work. However, as the example of LiCl points out, applying classical binding models to solvent exchange processes leads to well correlated but physically unrealistic results, because these models do not consider the effects of solvent exchange. On the other hand, the simple continuum model [17] provides a first principles description of the electrostatic interactions that occur when a formal unit of salt replaces a water molecule. The fact that the salt-induced stabilization of the protein is satisfactorily correlated with the predictions of theory indicates that it is likely that the description of the salt-induced electrostatic interactions is realistic. In other words, interactions between salt ions and their induced image charges in the protein medium are important contributors to the observed salt induced stability.

Understanding how salts influence protein stability has important implications, in the interpretation of protein structure, function and dynamics. Electrostatic interactions play an important role in stabilizing protein structure and can be the origin of many dynamic motions in proteins. Studying the effects of salts on various dynamic motions has been used to probe the roles these interactions play in the stability of proteins. However, until now, the major interpretation of salt effects has been based on how salts screen charge-charge interactions and often neglect salting-out effects caused by the interaction of salts and their induced image charges. Our results show the significance of these salting-out interactions in the stability of the protein folded state, pointing out that any analysis of salt effects on protein thermodynamics is incomplete without considering these interactions. In fact, neglecting salting-out effects may lead to overestimating (in the case of repulsive forces) or underestimating (in the case of attractive forces) the importance of various charge-charge interactions.

Finally, a better understanding of salting-out effects may also prove useful for understanding the thermodynamics of proteins associated with halophillic organisms. Extensive work on halophilic enzymes has demonstrated that the mechanisms by which salts affect halophilic and mesophilic variants of the same enzyme are similar in nature (e.g., charge–charge screening and Hofmeister effects) and are not specific to the halophile [40,46]. However, high concentrations of salt cause mesophilic enzymes to inactivate while halophilic enzymes are activated by high concentrations of salt. It is possible that this difference is caused by salting-out interactions having different effects on the mesophilic and halophilic proteins, meriting further study in this regard.

Acknowledgements

The authors would like to thank Professors Joe O'Neil, Jörg Stetefeld and Sean McKenna (University of Manitoba) for their comments regarding this manuscript.

References

[1] A. Wegner, G. Isenberg, 12-Fold difference between the critical monomer concentrations of the two ends of actin filaments in physiological salt conditions, Proceedings of the National Academy of Sciences of the United States of America 80 (1983) 4922–4925.
[2] T. Schlick, B. Li, W.K. Olson, The influence of salt on the structure and energetics of supercoiled DNA, Biophysical Journal 67 (1994) 2146–2166.
[3] R.L. Baldwin, How Hofmeister ion interactions affect protein stability, Biophysical Journal 71 (1996) 2056–2063.
[4] S.N. Timasheff, Solvent effects on protein stability, Current Opinion in Structural Biology 2 (1991) 35–39.
[5] Y. Zhang, P.S. Cremer, Interactions between macromolecules and ions: the Hofmeister series, Current Opinion in Chemical Biology 10 (2006) 658–663.
[6] J.G. Kirkwood, Acid–base equilibrium in solutions of ampholytes, Annals of the New York Academy of Sciences 41 (1941) 321–328.
[7] C. Tanford, J.G. Kirkwood, Theory of protein titration curves. I. General equations for impenetrable spheres, Journal of the American Chemical Society 79 (1957) 5333–5339.
[8] F. Dong, H.-X. Zhou, Electrostatic contributions to T4 lysozyme stability: solvent-exposed charges versus semi-buried salt bridges, Biophysical Journal 83 (2002) 1341–1347.
[9] Y.-H. Kao, C.A. Fitch, S. Bhattacharya, C.J. Sarkisian, J.T.J. Lecomte, B. Garcia-Moreno, E, Salt effects on ionization equilibria of histidines in myoglobin, Biophys J 79 (2000) 1637–1654.
[10] N.A. Simonov, M. Mascagni, M.O. Fenley, Monte Carlo-based linear Poisson–Boltzmann approach makes accurate salt-dependent solvation free energy predictions possible, Journal of Chemical Physics 127 (2007) 185105/185101-185105/185106.
[11] R. Geney, M. Layten, R. Gomperts, V. Hornak, C. Simmerling, Investigation of salt bridge stability in a generalized born solvent model, Journal of Chemical Theory and Computation 2 (2006) 115–127.
[12] J.D. Ballin, J.P. Prevas, C.R. Ross, E.A. Toth, G.M. Wilson, M.T. Record, contributions of the histidine side chain and the N-terminal α-amino group to the binding thermodynamics of oligopeptides to nucleic acids as a function of pH, Biochemistry 49 (2010) 2018–2030.

[13] B. Hribar, N.T. Southall, V. Vlachy, K.A. Dill, How ions affect the structure of water, Journal of the American Chemical Society 124 (2002) 12302–12311.
[14] A.S. Thomas, A.H. Elcock, Molecular dynamics simulations of hydrophobic associations in aqueous salt solutions indicate a connection between water hydrogen bonding and the Hofmeister effect, Journal of the American Chemical Society 129 (2007) 14887–14898.
[15] R. Piazza, Protein interactions and association: an open challenge for colloid science, Current Opinion in Colloid and Interface Science 8 (2004) 515–522.
[16] S. Finet, F. Skouri-Panet, M. Casselyn, F. Bonnete, A. Tardieu, The Hofmeister effect as seen by SAXS in protein solutions, Current Opinion in Colloid and Interface Science 9 (2004) 112–116.
[17] H.-X. Zhou, Interactions of macromolecules with salt ions: an electrostatic theory for the Hofmeister effect, Proteins: Structure, Function, and Bioinformatics 61 (2005) 69–78.
[18] X. Huang, H.-X. Zhou, Similarity and difference in the unfolding of thermophilic and mesophilic cold shock proteins studied by molecular dynamics simulations, Biophysical Journal 91 (2006) 2451–2463.
[19] S. Spencer Daniel, K. Xu, M. Logan Timothy, H.-X. Zhou, Effects of pH, salt, and macromolecular crowding on the stability of FK506-binding protein: an integrated experimental and theoretical study, Journal of Molecular Biology 351 (2005) 219–232.
[20] J. Steyaert, A decade of protein engineering on ribonuclease T1. Atomic dissection of the enzyme–substrate interactions, European Journal of Biochemistry 247 (1997) 1–11.
[21] C.N. Pace, U. Heinemann, U. Hahn, W. Saenger, Ribonuclease T1: structure, function and stability, Angewandte Chemie 103 (1991) 351–369 (See also Angew Chem , Int Ed Engl , 1991, 1930(1994), 1343–1960).
[22] H. Yoshida, The ribonuclease T1 family, Methods in Enzymology 341 (2001) 28–41.
[23] D.L. Beauchamp, M. Khajehpour, Probing the effect of water–water interactions on enzyme activity with salt gradients: a case-study using ribonuclease t1, The Journal of Physical Chemistry. B 114 (2010) 16918–16928.
[24] J.M. Scholtz, G.R. Grimsley, C.N. Pace, Solvent denaturation of proteins and interpretations of the M value, Methods in Enzymology 466 (2009) 549–565.
[25] C.N. Pace, Determination and analysis of urea and guanidine hydrochloride denaturation curves, Methods in Enzymology 131 (1986) 266–280.
[26] M.M. Santoro, D.W. Bolen, Unfolding free energy changes determined by the linear extrapolation method. 1. Unfolding of phenylmethanesulfonyl alpha - chymotrypsin using different denaturants, Biochemistry 27 (1988) 8063–8068.
[27] J.R. Lakowicz, Principles of Fluorescence Spectroscopy, (1983).
[28] S.L.C. Moors, A. Jonckheer, M. De Maeyer, Y. Engelborghs, A. Ceulemans, Tryptophan conformations associated with partial unfolding in ribonuclease T1, Biophysical Journal 97 (2009) 1778–1786.
[29] M.C.R. Shastry, M.R. Eftink, Reversible thermal unfolding of ribonuclease T1 in reverse micelles, Biochemistry 35 (1996) 4094–4101.
[30] M. Ruoppolo, R.B. Freedman, Refolding by disulfide isomerization: the mixed disulfide between ribonuclease T1 and glutathione as a model refolding substrate, Biochemistry 34 (1995) 9380–9388.
[31] B. Somogyi, M. Punyiczki, J. Hedstrom, J.A. Norman, F.G. Prendergast, A. Rosenberg, Coupling between external viscosity and the intramolecular dynamics of ribonuclease T1: a two-phase model for the quenching of protein fluorescence, Biochimica et Biophysica Acta, Protein Structure and Molecular Enzymology 1209 (1994) 61–68.
[32] Y. Yamamoto, J. Tanaka, Spectroscopic studies on the configurational structures of ribonuclease T1, Biochimica et Biophysica Acta, Protein Structure 207 (1970) 522–531.
[33] C.Q. Hu, J.M. Sturtevant, J.A. Thomson, R.E. Erickson, C.N. Pace, Thermodynamics of ribonuclease T1 denaturation, Biochemistry 31 (1992) 4876–4882.
[34] C.N. Pace, G.R. Grimsley, Ribonuclease T1 is stabilized by cation and anion binding, Biochemistry 27 (1988) 3242–3246.
[35] C.N. Pace, D.V. Laurents, J.A. Thomson, pH dependence of the urea and guanidine hydrochloride denaturation of ribonuclease A and ribonuclease T1, Biochemistry 29 (1990) 2564–2572.
[36] J. Deswarte, S. De Vos, U. Langhorst, J. Steyaert, R. Loris, The contribution of metal ions to the conformational stability of ribonuclease T1. Crystal versus solution, European Journal of Biochemistry 268 (2001) 3993–4000.
[37] J.A. Thomson, B.A. Shirley, G.R. Grimsley, C.N. Pace, Conformational stability and mechanism of folding of ribonuclease T1, Journal of Biological Chemistry 264 (1989) 11614–11620.
[38] M.A. de los Rios, K.W. Plaxco, Apparent Debye–Huckel electrostatic effects in the folding of a simple, single domain protein, Biochemistry 44 (2005) 1243–1250.
[39] B. Song, J.-H. Cho, D.P. Raleigh, Ionic-strength-dependent effects in protein folding: analysis of rate equilibrium free-energy relationships and their interpretation, Biochemistry 46 (2007) 14206–14214.
[40] L.M. Gloss, B.J. Placek, The effect of salts on the stability of the H2A–H2B histone dimer, Biochemistry 41 (2002) 14951–14959.
[41] M. Itaya, Y. Inoue, Steady-state kinetic studies of the inhibitory action of zinc on ribonuclease T1 catalysis, Biochemistry Journal 207 (1982) 357–362.
[42] K. Takahashi, T. Uchida, F. Egami, Ribonuclease T1, structure and function, Advances in Biophysics 1 (1970) 53–98.
[43] M. Vijayakumar, M.S. Gopinathan, Pair correlation energies and successive ionization potentials of atoms helium through zinc, Journal of Chemical Physics 97 (1992) 6639–6643.
[44] T. Liu, P.R. Callis, B.H. Hesp, M. de Groot, W.J. Buma, J. Broos, Ionization potentials of fluoroindoles and the origin of nonexponential tryptophan fluorescence decay in proteins, Journal of the American Chemical Society 127 (2005) 4104–4113.
[45] J. Ding, H.W. Choe, J. Granzin, W. Saenger, Structure of ribonuclease T1 complexed with zinc(II) at 1.8 Å resolution: a Zn2+.6H2O.carboxylate clathrate, Acta Crystallographica Section B: Structural Science B48 (1992) 185–191.
[46] L.M. Gloss, T.B. Topping, A.K. Binder, J.R. Lohman, Kinetic folding of Haloferax volcanii and Escherichia coli dihydrofolate reductases: haloadaptation by unfolded state destabilization at high ionic strength, Journal of Molecular Biology 376 (2008) 1451–1462.
[47] J.A. Schellman, The thermodynamics of solvent exchange, Biopolymers 34 (1994) 1015–1026.
[48] J.A. Schellman, Protein stability in mixed solvents: a balance of contact interaction and excluded volume, Biophysical Journal 85 (2003) 108–125.
[49] S.N. Timasheff, Thermodynamic binding and site occupancy in the light of the Schellman exchange concept, Biophysical Chemistry 101–102 (2002) 99–111.
[50] H.-X. Zhou, F. Dong, Electrostatic contributions to the stability of a thermophilic cold shock protein, Biophysical Journal 84 (2003) 2216–2222.
[51] J. Srinivasan, M.W. Trevathan, P. Beroza, D.A. Case, Application of a pairwise generalized born model to proteins and nucleic acids. Inclusion of salt effects, Theoretical Chemistry Accounts 101 (1999) 426–434.
[52] Z. Abbas, M. Gunnarsson, E. Ahlberg, S. Nordholm, Corrected Debye–Hueckel theory of salt solutions: size asymmetry and effective diameters, The Journal of Physical Chemistry. B 106 (2002) 1403–1420.
[53] S. Bykov, S. Asher, Raman studies of solution polyglycine conformations, The Journal of Physical Chemistry. B 114 (2010) 6636–6641.
[54] A.S. Thomas, A.H. Elcock, Molecular dynamics simulations predict a favorable and unique mode of interaction between lithium (Li+) ions and hydrophobic molecules in aqueous solution, Journal of Chemical Theory and Computation 7 (2011) 818–824.
[55] W.K. Lim, J. Rosgen, S.W. Englander, Urea, but not guanidinium, destabilizes proteins by forming hydrogen bonds to the peptide group, Proceedings of the National Academy of Sciences of the United States of America 106 (2009) 2595–2600.
[56] C.F. Baes Jr., R.E. Mesmer, The Hydrolysis of Cations, (1976).